

## Muonium states in HgO

This article has been downloaded from IOPscience. Please scroll down to see the full text article.

2001 J. Phys.: Condens. Matter 13 L613

(<http://iopscience.iop.org/0953-8984/13/27/101>)

View [the table of contents for this issue](#), or go to the [journal homepage](#) for more

Download details:

IP Address: 171.66.16.226

The article was downloaded on 16/05/2010 at 13:52

Please note that [terms and conditions apply](#).

## LETTER TO THE EDITOR

**Muonium states in HgO**

**J M Gil<sup>1</sup>, H V Alberto<sup>1</sup>, R C Vilão<sup>1</sup>, J Piroto Duarte<sup>1</sup>,  
N Ayres de Campos<sup>1</sup>, A Weidinger<sup>2</sup>, E A Davis<sup>3</sup> and S F J Cox<sup>4</sup>**

<sup>1</sup> Physics Department, University of Coimbra, P-3004-516 Coimbra, Portugal

<sup>2</sup> Hahn-Meitner Institut Berlin, Glienicke Strasse 100, D-14109 Berlin, Germany

<sup>3</sup> Department of Physics and Astronomy, University of Leicester, Leicester LE1 7RH, UK

<sup>4</sup> ISIS Facility, Rutherford Appleton Laboratory, Chilton OX11 0QX, UK

Received 29 March 2001, in final form 23 May 2001

Published 22 June 2001

Online at [stacks.iop.org/JPhysCM/13/L613](http://stacks.iop.org/JPhysCM/13/L613)

**Abstract**

Experimental data on muonium states in HgO are presented. Muon spin rotation ( $\mu$ SR) experiments show that, at low temperatures, approximately 80% of muons implanted into a polycrystalline sample form paramagnetic centres with hyperfine interaction parameters  $A_{\text{iso}} = 14.93(5)$  MHz and  $D = 5.2(1)$  MHz. The remaining 20% form diamagnetic states. Diffusion of the paramagnetic state through equivalent sites is observed above 10 K, averaging the apparent anisotropy to a low value at and above 50 K. The variations of the amplitudes of the two signals with temperature indicate that the paramagnetic centres ionize in a temperature range centred around 160 K and that the associated donor levels lie considerably further from the conduction band edge than the corresponding states in ZnO and other II–VI compounds.

**1. Introduction**

The analogy that has been established between muonium (Mu, or  $\mu^+e^-$ ) and the isolated hydrogen atom prompted the extensive use of muon-spin research for the indirect study of hydrogen in semiconductors [1]. In this context muonium states in elemental and III–V compound semiconductors have been identified and studied to a great extent. Charged states  $\text{Mu}^+$  and  $\text{Mu}^-$  and two forms of the neutral state  $\text{Mu}^0$  have been identified and the interplay of site and charge states is understood [2].  $\text{Mu}^0$  can either be isotropic, when in a symmetric interstitial site such as the tetrahedral site in diamond or zincblende structures ( $\text{Mu}_T^0$ ), or anisotropic when situated at the bond-centre site ( $\text{Mu}_{\text{BC}}^0$ ). In these semiconductors, isolated H and Mu are known to form deep-level centres.

More recently, studies of Mu in II–VI semiconductors revealed the existence of a third form of neutral anisotropic  $\text{Mu}^0$  in CdS, CdSe, CdTe and ZnO [3–5]. This state has binding energies characteristic of shallow-level donor centres and is believed to be at the interstitial site anti-bonding to S (Se, Te, or O). Its hyperfine interaction is very weak, amounting to approximately  $10^{-4}$  of the free-atom value. Theoretical work that predicted the existence of a

shallow-level state associated with hydrogen in ZnO [6] suggests that a search in other oxides might be fruitful.

We present here the first results of a muon spin rotation ( $\mu$ SR) study of muonium states in another oxide of the II–VI family, namely the wide-gap semiconductor HgO, which has an orthorhombic structure and a band gap of 2.19 eV. A new form of anisotropic muonium, with hyperfine constant intermediate between those of the shallow-level states of CdS and ZnO and those of the deep levels in other semiconductors, is found.

## 2. Experimental details

Conventional transverse-field arrangements were used in the  $\mu$ SR experiments. By measuring the spatial asymmetry of the emission of positrons from the decay of muons implanted into the sample, the time development of the muon spin polarization is recorded. The different muonium states formed in the sample are distinguished in these time spectra by characteristic spin precession frequencies revealing the presence of each muonium species and characterizing the hyperfine parameters of paramagnetic muonium states.

The samples consisted of commercially available (from AlfaAesar) polycrystalline Hg(II)O of the highest purity available (99.998%), with an orthorhombic crystalline structure. The data presented in this letter were obtained at the Paul Scherrer Institute in Switzerland, using the GPS instrument. Additional measurements in longitudinal magnetic field, made at the ISIS Facility in the United Kingdom, support the present spectroscopic interpretation and give additional information on dynamics; these will be presented in a fuller account elsewhere.

## 3. Results

Transverse-field measurements were performed at different temperatures at 0.4 T. Figure 1 presents, as an example, the time spectrum obtained at 2 K and the respective Fourier transform. The central sharp line corresponds to the Larmor precession of the diamagnetic fraction of implanted muons. The satellite frequency distributions, symmetric in shape and position relative to the central line, correspond to the transitions expected in the Paschen–Back régime for a paramagnetic state. The separation of the satellite lines is directly related to the hyperfine constant of this neutral muonium state and their width is attributed to a distribution of precession frequencies for each transition, which for an anisotropic state with axial symmetry are dependent on the angle between the symmetry axis of the hyperfine tensor and the applied external field. This width is directly related to the anisotropy parameter  $D$  of the hyperfine interaction tensor.

For axial symmetry, the anisotropic hyperfine tensor has principal elements  $A_{\parallel}$ , parallel to the symmetry axis, and  $A_{\perp}$ , perpendicular to this axis. An equivalent description of the hyperfine interaction expresses it as a combination of an isotropic and a traceless dipolar term. The isotropic part is given by  $A_{\text{iso}} = \frac{1}{3}(A_{\parallel} + 2A_{\perp})$  whereas the dipolar tensor is described by the asymmetry parameter  $D = \frac{2}{3}(A_{\parallel} - A_{\perp})$ , yielding the hyperfine interaction  $A$  as a function of angle  $\theta$  between the symmetry axis and the direction of the external field [7]:

$$A = A_{\text{iso}} + \frac{D}{2}(3 \cos^2 \theta - 1). \quad (1)$$

This expression holds in the Paschen–Back region. From orientation-dependent measurements on single crystals, both the hyperfine interaction parameters and the direction of the symmetry axis can be derived. For a polycrystalline sample, the principal values of the tensor are accessible but not the crystallographic direction of its symmetry axis, since this is oriented

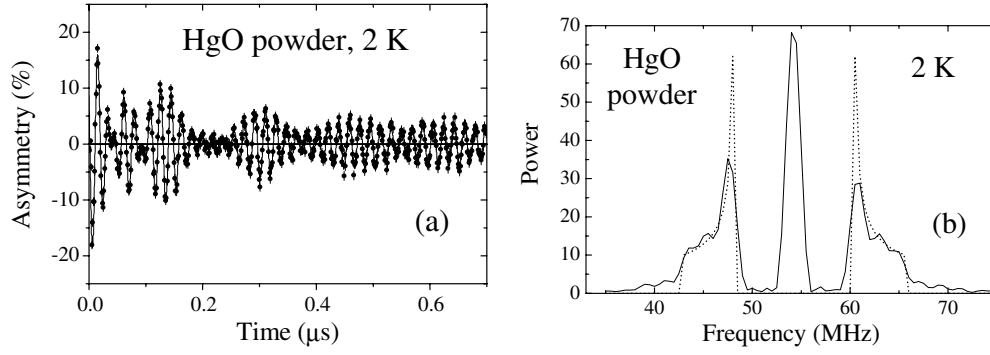


**Figure 1.** Transverse-field time spectrum (a) and frequency spectrum (b) obtained for HgO powder at an external field of 0.4 T and at 2 K. The full curve in (a) is the fitted function according to equation (3) with a Lorentzian folding. The dashed curve in (b) corresponds to the frequency distribution of equation (2) with the fitted parameters and without any folding.

randomly relative to the external field, within the range of  $\theta$  from 0 to  $\pi/2$ . As a consequence of this random orientation, the observed splitting is composed of a frequency distribution, characterized by an average value ( $A_{\text{iso}}$ ) and a width (proportional to  $D$ ). The following expression is derived for the probability density of the frequency distribution  $dP/d\nu$ :

$$\frac{dP}{d\nu} = \frac{dP}{d\theta} \frac{d\theta}{d\nu} = (3D)^{-1/2} (2(|\nu - \nu_0| - A_{\text{iso}}) + D)^{-1/2} \quad (2)$$

for

$$\nu_0 - A_{\parallel}/2 \leq \nu \leq \nu_0 - A_{\perp}/2 \quad \text{and} \quad \nu_0 + A_{\perp}/2 \leq \nu \leq \nu_0 + A_{\parallel}/2$$

where  $\nu_0$  is the centre of the frequency distribution.

The probability  $P_i$  associated with a narrow frequency interval centred on  $\nu_i$  can be derived from the previous equation, and a time-dependent polarization function for muonium can then be expressed as a weighted sum:

$$f_{\text{Mu}}(t) = \sum_i P_i(A_{\text{iso}}, D, \nu_0) \cos(2\pi \nu_i t + \phi). \quad (3)$$

A least-squares fitting was performed using a cosine function for the central diamagnetic line and frequency distributions according to equation (3) for the satellite lines, with  $A_{\text{iso}}$ ,  $D$  and the centre of the distribution as fit parameters. A Lorentzian folding was also considered on both components in the fitting procedure. The values obtained from such a fit to the time spectrum obtained at 2 K (figure 1(a)) were  $A_{\text{iso}} = 14.93(5)$  MHz,  $D = 5.2(1)$  MHz and a central frequency that is equal to that of diamagnetic muons within the experimental error. The value obtained in the fit for the width of the Lorentzian folding function of the paramagnetic component is of the order of  $3 \mu\text{s}^{-1}$ , and is attributed to other interactions not considered in the model of equations (2) and (3), such as the interaction with the odd-spin neighbouring nuclei or spin-exchange with charge carriers. The dashed curves in figure 1(b) represent the frequency distribution obtained with equation (2) and the parameters obtained in the fit to the time-domain spectrum, without any folding. The relative paramagnetic fraction was found to be 82(2)%.

Measurements at increasing temperatures reveal a strong narrowing of the frequency distribution of the satellite lines as can be seen in figure 2(a), where the Fourier transform of the time spectrum obtained at 50 K is presented. The described fitting procedure was applied to the data at all measured temperatures. An effective asymmetry parameter  $D_{\text{eff}}$

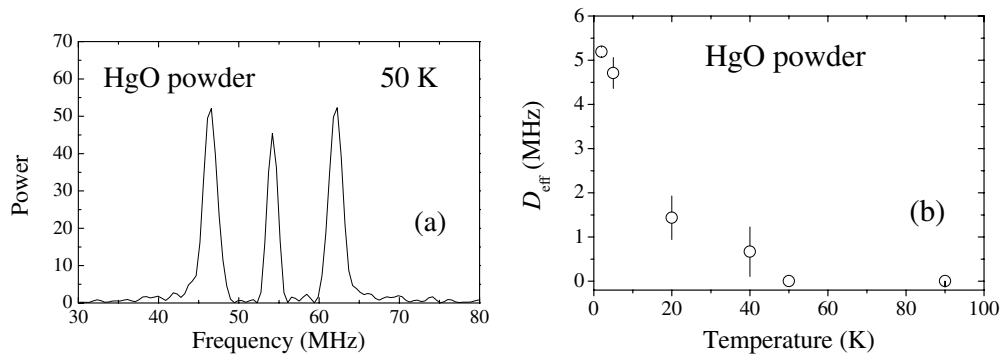


**Figure 2.** (a) Frequency spectrum obtained with HgO powder in a transverse-field of 0.4 T and at 50 K. (b) The narrowing of the width of the satellite lines (compare (a) with figure 1(b)) is expressed in the fitting by the effective asymmetry parameter  $D_{\text{eff}}$ , here presented as a function of measuring temperature.

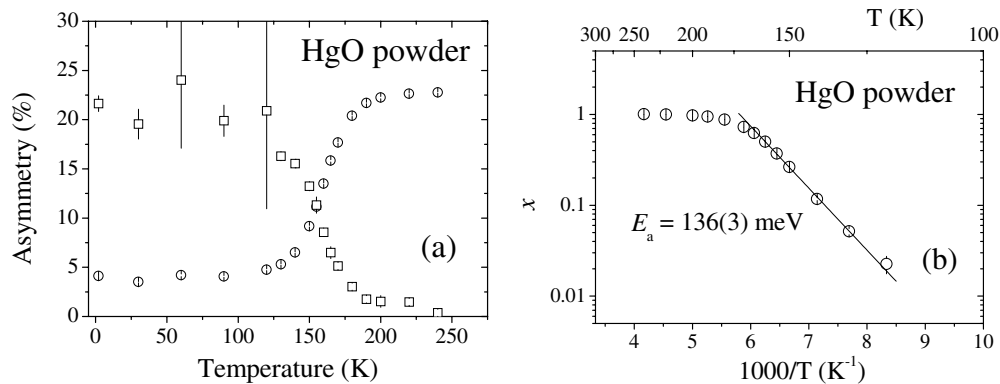


**Figure 3.** (a) Variation with temperature of the oscillating amplitude of the diamagnetic ( $\circ$ ) and paramagnetic ( $\square$ ) fractions of muons implanted in HgO powder, as seen in transverse-field measurements at 0.01 T. (b) An Arrhenius plot for the increase of the fraction of ionized states. The slope of the best-fit line is  $E_a = 136(3)$  meV.

could be obtained with values decreasing with increasing temperature, reaching  $0.002 \mu\text{s}^{-1}$  at 50 K (see figure 2(b)). Equally low  $D_{\text{eff}}$  values are obtained above 50 K. The spectral weights of the diamagnetic and paramagnetic fractions, as well as the folding widths, remain constant through the temperature range corresponding to the narrowing of  $D_{\text{eff}}$ .

Above 120 K a decrease in the amplitude of the paramagnetic signal is observed, as the amplitude of the diamagnetic fraction increases correspondingly. Additional measurements were performed in that range of temperatures. The applied transverse field was 0.01 T. Although this field is not in the Paschen–Back régime, least-squares fits with cosine functions of the Gaussian envelope reveal the presence of the paramagnetic fraction in the form of two broad frequency lines centred at 4.5 and 7.5 MHz (for the 2 K data), besides the Larmor diamagnetic line. The relative fractions are the same as observed at 0.4 T.

The same fitting procedure was used for the analysis of the spectra accumulated at different temperatures between 2 and 240 K, with the same applied field of 0.01 T. The separation of the diamagnetic and paramagnetic fractions is very clear at all temperatures and the diamagnetic fraction amplitude is determined within a small experimental error. The

variation with temperature of the amplitudes of the diamagnetic and the paramagnetic fractions is shown in figure 3(a). The diamagnetic fraction amplitude shows a large increase centred around 160 K, up to a full oscillating amplitude at 240 K. The amplitude of the paramagnetic fraction decreases correspondingly to zero above 200 K. This behaviour provides evidence of ionization of the paramagnetic muonium state.

Figure 3(b) shows an Arrhenius plot of the fraction of ionized states against inverse temperature. An activation energy of  $E_a = 136(3)$  meV for the ionization process is determined by fitting a straight line to the data.

#### 4. Discussion

The existence in HgO of a paramagnetic state of muonium with an associated ionization energy of about 136 meV stands in contrast to the paramagnetic states found in ZnO, CdS, CdSe and CdTe, for which much lower ionization energies have been found corresponding to shallower centres [3–5]. The hyperfine constants for the anisotropic hyperfine interaction of the paramagnetic state,  $A_{\text{iso}} = 14.93(5)$  MHz and  $D = 5.2(1)$  MHz, can be compared with those of the bond-centre states ( $\text{Mu}_{\text{BC}}^0$ ) in Si, namely  $A_{\text{iso}} = 67$  MHz and  $D = 51$  MHz, or in Ge,  $A_{\text{iso}} = 96$  MHz and  $D = 69$  MHz [7]. A comparison can also be made for the ionization energies, which are 220 meV and 230 meV for  $\text{Mu}_{\text{BC}}^0$  in Si [8] and in Ge [9], respectively. In these two semiconductors, the muon sits at the centre of a covalent bond with the associated electron having maximal probability amplitudes at the two adjacent atoms lying in the bond direction but on opposite sides of the Si or Ge atoms [10, 11].

It would, however, be premature to assign the paramagnetic centre in HgO to the BC site because the material has an orthorhombic structure and its atoms are not tetrahedrally coordinated as in the group-IV semiconductors. Furthermore, the bonding between Hg and O is partially ionic and a symmetric site does not exist between the atoms as in Si or Ge, or in some III–V compounds. Alternative sites with the required axial symmetry are anti-bonding sites of the O atoms. Indeed, angle-dependent studies on single crystals of CdS were used to identify the anti-bonding sites of S as likely candidates for the location of the paramagnetic centres in this material [3, 5]. However, we have not as yet been able to obtain single crystals of HgO on which to perform similar studies and, in any case, the hyperfine parameters for CdS differ considerably from those found here for HgO.

The narrowing of the powder frequency distribution of this anisotropic state is attributed to the effect of diffusion through equivalent, or almost equivalent, sites in the orthorhombic HgO structure. If the time of stay at a particular site is of the order of  $\Delta\nu^{-1} = 4(3D)^{-1} = 0.3 \mu\text{s}$  with  $\Delta\nu$  corresponding to the frequency spread at low temperatures, motional narrowing sets in. Then, the asymmetry parameter averages to an effective lower value  $D_{\text{eff}}$  (see figure 2(b)), while the centre of the frequency distribution stays the same. Experimentally (see figure 2(b)) the half value of  $D_{\text{eff}}$  occurs around 15 K, suggesting a mean time of stay at this temperature of the order of  $0.3 \mu\text{s}$ . A more detailed study of this effect with additional measurements both in transverse and longitudinal fields is expected to lead to the determination of diffusion parameters of the paramagnetic muonium state in this compound.

The discovery of a new type of centre with values of contact interaction and ionization energy lying between those associated with muonium in other II–VI compounds, on the one hand, and in the group-IV semiconductors, on the other, is a significant result which merits further experimental and theoretical investigations.

This work was partially supported by the POCTI programme (FCT funding and project POCTI/35334/FIS/2000, Portugal), and EPSRC grant GMM0041 (UK).

## References

- [1] Chow K H, Hitti B and Kiefl R F 1998 *Identification of Defects in Semiconductors (Semiconductors and Semimetals 51A)* ed M Stavola (New York: Academic) p 137
- [2] Lichti R L 1999 *Hydrogen in Semiconductors II (Semiconductors and Semimetals 61)* ed N H Nickel (New York: Academic) p 311
- [3] Gil J M *et al* 1999 *Phys. Rev. Lett.* **83** 5294
- [4] Cox S F J *et al* 2001 *Phys. Rev. Lett.* **86** 2601
- [5] Gil J M, Alberto H V, Vilão R C, Pioto Duarte J, Ayres de Campos N, Weidinger A, Krauser J, Davis E A, Cottrell S P and Cox S F J 2001 *Phys. Rev. B*, at press
- [6] Van de Walle C G 2000 *Phys. Rev. Lett.* **85** 1012
- [7] Patterson B D 1988 *Rev. Mod. Phys.* **60** 69
- [8] Lichti R L 1995 *Phil. Trans. R. Soc. A* **350** 323
- [9] Lichti R L, Cox S F J, Chow K H, Davis E A, Estle T L, Hitti B, Mytilineou E and Schwab C 1999 *Phys. Rev. B* **60** 1734
- [10] Cox S F J and Symons M C R 1986 *Chem. Phys. Lett.* **126** 516
- [11] Kiefl R F, Celio M, Estle T L, Kreitzman S R, Luke G M, Riseman T M and Ansaldo E J 1988 *Phys. Rev. Lett.* **60** 224